Chapter 10

Magnetosphere Ionosphere Coupling and Substorms

10.1 Magnetosphere-Ionosphere Coupling

10.1.1 Currents and Convection in the Ionosphere

The coupling between the magnetosphere and the ionosphere is important because (1) there is a large amount of energy deposited in the ionosphere and (2) the ionosphere provides in addition to the solar wind the only boundary to the magnetosphere.

Convection in the magnetosphere is illustrated in Figure 10.1. For southward IMF the convection is predominantly driven by reconnection at the dayside magnetopause. The newly reconnected magnetic flux is convected over the polar caps and added to the magnetotail lobes. Reconnection in the magnetotail then closes the flux again and the closed magnetic flux is transported azimuthally around the Earth to the dayside to restart the cycle. Note that this is a time averaged and strongly simplified model but is well suited to illustrate the coupling aspects.

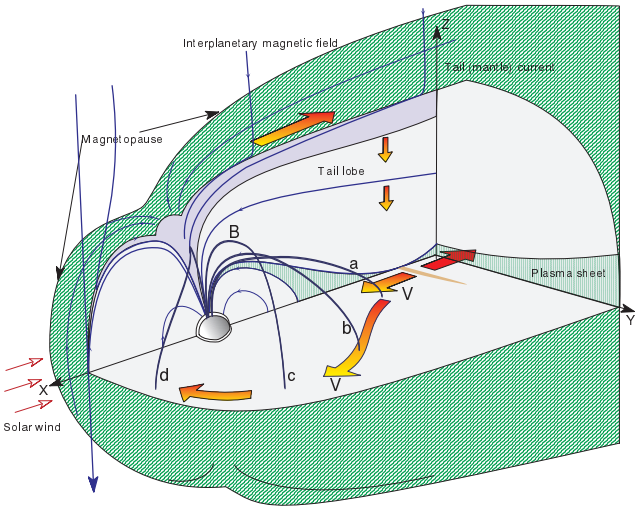

Figure 10.1: Illustration of convection in the magnetosphere.

Traditionally magnetosphere - ionosphere coupling assumes a stationary state. In this case $\partial \mathbf{B}/\partial t = \nabla \times \mathbf{E} = 0$ implies that the electric field can be derived from a potential

$$\begin{aligned} \mathbf{E} &= -\nabla\phi \\ \text{and} \qquad & \mathbf{E} \cdot \mathbf{B} = 0 \end{aligned}$$

implies that this potential is constant on magnetic field lines and maps into the ionosphere. This also implies that from the electric field he perpendicular velocity is given by $\mathbf{v}_\perp = \mathbf{E} \times \mathbf{B}/\mathbf{B}^2$. Because of the large phase velocity of the fast wave in the ionosphere, the ionospheric flow is largely incompressible. Since the electric field is caused by convection, contour lines of the potential are flow lines in the ionosphere.

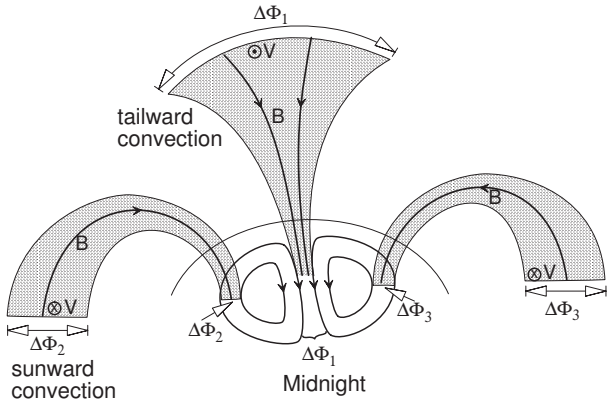

Figure 10.2: Illustration of the mapping of magnetospheric convection into the ionosphere.

Figure 10.2 illustrates the mapping from the magnetosphere into the ionosphere. Magnetic flux reconnected at the dayside magnetopause is convected tailward. The potential $\Delta\Phi_1$due to convection from the dayside to the nightside matches the potential in the ionosphere. Similarly the return flow at lower latitudes maps into the ionosphere. The typical ionospheric convection velocities can be derived through the mapping of the magnetic field.

Conservation of magnetic flux for a flux tube with cross sectional area $A = L^2$

$$\int_A \mathbf{B} \cdot d\mathbf{s} = const$$

implies $B_{io}L_{io}^2 = B_{msp}L_{msp}^2$

such that $L_{io}/L_{msp} = \sqrt{B_{msp}/B_{io}}$

for a sufficiently small flux tube. This implies for the electric field and velocity mapping

$$\begin{aligned} \frac{E_{io}}{E_{msp}} &= \frac{\Delta\phi/L_{io}}{\Delta\phi/L_{msp}} = \sqrt{B_{io}/B_{msp}} \\ \frac{v_{\perp io}}{v_{msp}} &= \frac{E_{io}/B_{io}}{E_{msp}/B_{msp}} = \sqrt{B_{msp}/B_{io}} \end{aligned}$$

Using typical values (for the dayside magnetospheric boundary): $v_{io} \approx 1$ km/s, $B_{io} \approx 4 \times 10^{-5}$ T, and $B_{msp} \approx 10^{-8}$ T

yields $L_{io}/L_{msp} \approx 1/60$, $v_{msp} \approx 60$ km/s

$E_{io} \approx 40$ mV/m, $E_{msp} \approx 0.7$ mV/m

The total cross polar cap potential is typically a few 10 kV with larger values of 50 to 70 kV for southward IMF. Extreme condition can lead of polar cap potentials slightly larger than 100kV. For strongly northward IMF the convection actually assumes a 4 cell pattern with sunward convection in the dayside polar cap and anti-sunward convection on the nightside. This dayside convection is driven by reconnection in the magnetospheric cusps.

Often the concept of magnetic flux transport appears somewhat abstract. To provide an example, let us consider a surface $\mathbf{A}$ as illustrated in Figure 10.3. Assuming that the velocity at all boundaries of this surface is only tangential except for the line $\overline{ab}$ where we consider a velocity pointed into the surface $\mathbf{A}$. The magnetic flux through the area $\mathbf{A}$ is

$$\Phi = \int_{\mathbf{A}} \mathbf{B} \cdot d\mathbf{s}$$

and the change of the magnetic flux is then

$$\begin{aligned} \frac{d\Phi}{dt} &= \int_{\mathbf{A}} \frac{\partial \mathbf{B}}{\partial t} \cdot d\mathbf{s} = -\int_{\mathbf{A}} (\nabla \times \mathbf{E}) \cdot d\mathbf{s} \\ &= -\oint_{\mathbf{A}} \mathbf{E} \cdot d\mathbf{l} = \phi_b - \phi_a \end{aligned}$$

or $d\Phi/dt = \Delta\phi$. This example illustrates that the cross polar cap potential indeed represents the magnetic flux transported from the dayside magnetosphere to the night side.

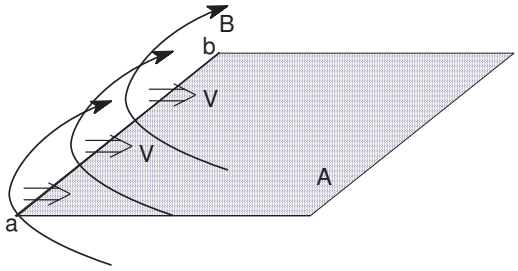

Figure 10.3: Illustration of magnetic flux transport.

At the dayside this flux transport is initiated through magnetic reconnection. Assuming that there is a single magnetic X-line of length With an electric field $\mathbf{E}_{xl}$ at this line the reconnected flux (flux that is connected from the IMF to geomagnetic flux) per unit time is

$$\left.\frac{d\Phi}{dt}\right|_{\mathbf{X\,line}} = -\int_{\mathbf{X\,line}} \mathbf{E}_{xl} \cdot d\mathbf{l}$$

This X-line represents also the open closed magnetic boundary and should map into the ionosphere approximately at the location where the ionospheric plasma undergoes an anti-sunward acceleration.

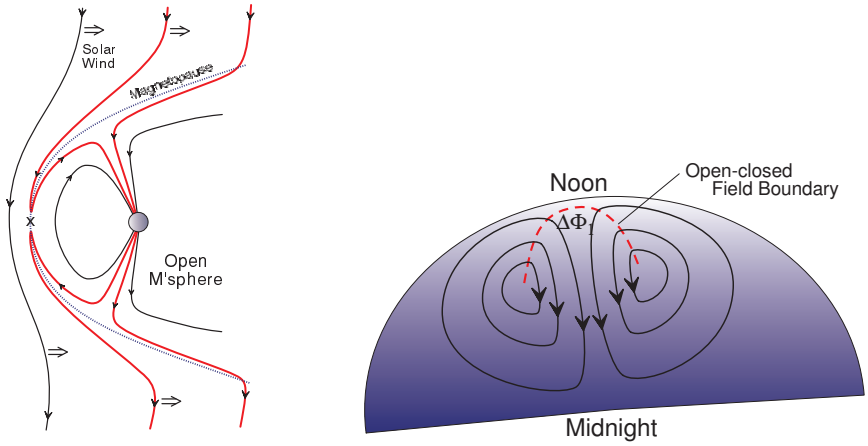

Figure 10.4: Dayside reconnection and corresponding convection in the ionosphere.

As pointed out, this picture assumes a time averaged state or a stationary state both of which are approximations. This mapping of magnetospheric convection is violated for two basic conditions;

(a) For time dependent processes $\partial/\partial t \neq 0$, e.g.,

- magnetospheric processes faster than the MI coupling time (n Alfvén transit times with n depending on the conductance);
- large scale nonsteady magnetospheric evolution;
- compressible magnetospheric processes;
  - Ionosphere: $\nabla \cdot \mathbf{v} = 0$
  - Magnetosphere: $\nabla \cdot \mathbf{v} \neq 0$

(b) For electric field parallel to the magnetic field ($E_{\parallel} = 0$)

- field-aligned electric fields;
- onset of strong precipitation;

It is obvious that both of these types of violations occur. Let us first consider the aspect of time dependence. To qualify this we need to understand the time scale of the coupling between the magnetosphere and ionosphere. The dominant mechanism for this coupling is the propagation of Alfvén waves. Let us assume a temporal change in the convection in the magnetosphere. This change in convection is traveling along magnetic field lines, i.e., the change in the perpendicular velocity (or equivalent electric field) is communicated through an Alfvén wave carrying the corresponding velocity (or electric field) change along field lines in the magnetosphere. However, the ionosphere is a conducting medium which implies that the wave once it arrives in the ionosphere is partially reflected depending on the ionospheric conductance.

Let us examine this reflection by assuming and incoming infinite wave train with fixed amplitude $\delta B_y = B_i$ and $\delta v_y = v_i = \frac{B_i}{B_x} v_A$ traveling into the negative z direction as illustrated in Figure 10.5. The reflected wave has the amplitudes$\delta B_y = B_o$ and $\delta v_y = v_o = -\frac{B_o}{B_x} v_A$ for the magnetic field and

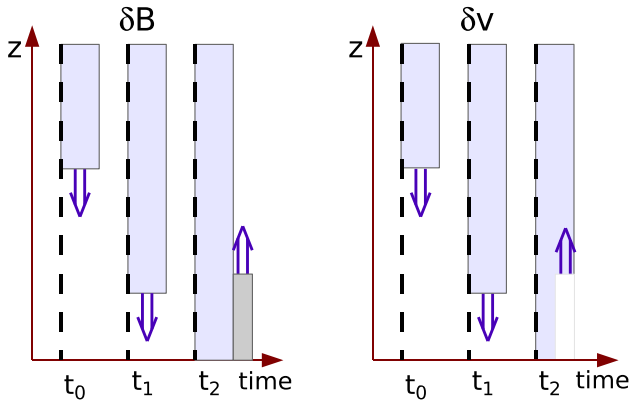

Figure 10.5: Reflection of Alfvén waves from the ionosphere.

velocity. Note that the magnetic field perturbation is in the same direction as for the incoming wave whereas the velocity perturbation is in the opposite direction (note that the wave vector $\mathbf{k}$ is in the opposite direction. The superposition of incoming and reflected waves yields the height integrated ionospheric current which is related to the electric field in the ionosphere through the conductance

$$\begin{aligned} I_{p,z} = \frac{1}{\mu_0}\left(B_i + B_o\right) &= \Sigma_p\left(E_{z,i} + E_{z,o}\right) \\ &= \Sigma_p B_x\left(v_i + v_o\right) \end{aligned}$$

Substitution for v_i and v_o using the relation between velocity and magnetic perturbation for Alfvén waves yields

$$\begin{aligned} B_i + B_o &= \mu_0 v_A \Sigma_p\left(B_i - B_o\right) \\ &or \\ B_o &= \frac{\mu_0 v_A \Sigma_p - 1}{\mu_0 v_A \Sigma_p + 1} B_i \end{aligned}$$

This yields the reflection coefficient for Alfvén waves

$$r = \frac{\Sigma_p - 1/\left(\mu_0 v_A\right)}{\Sigma_p + 1/\left(\mu_0 v_A\right)}$$

Here $1/\left(\mu_0 v_A\right)$ is the Alfvénic impedance. The basic time scale is the Alfvén transit time between the magnetosphere and ionosphere $\tau_A = \int_{msp}^{io} ds/v_A(s) \approx 2$ min. With the height integrated conductivity: $\Sigma_p \approx 20$ S (daytime & active), 2 S (night, quiet), and the Alfvén impedance of $\Sigma_A \approx 2$ S (daytime & active), 1 S (night, quiet) the reflection coefficient is

$$r = \begin{cases} > 0.8 & day\,\&\,active \\ 0.3 & night,\ quiet \end{cases}$$

The resulting total magnetic and velocity perturbations after a single reflection are

$$\begin{aligned} \frac{\delta B_i + \delta B_o}{\delta B_i} &= r + 1 \\ \frac{\delta v_i + \delta v_o}{\delta v_i} &= 1 - r \end{aligned}$$

which implies specifically that for a large ionospheric conductance it may take up to 10 Alfvén transit times to accelerate the ionospheric plasma to 90% of the velocity corresponding to an approximate steady state.

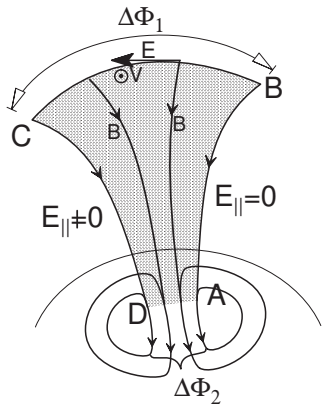

Figure 10.6: Mapping in the presence of a parallel electric field component.

The presence of a parallel electric field is the second issue that can alter the interpretation of the ionospheric convection regarding magnetic flux transport in the magnetosphere. Figure 8.3 illustrates the situation. Assuming a steady state with $E_\parallel \neq 0$ along the field line $\mathbf{BC}$ with

$$\phi_\parallel = \int_{\mathbf{CD}} E_\parallel dl$$

implies for a steady state $\phi_1 + \phi_\parallel - \phi_2 = 0$ or

$$\phi_2 = \phi_1 + \phi_\parallel$$

In principle the difference between the magnetospheric and the ionospheric flux transport can thus be determined if we know $\phi_\parallel$. Since an electric field parallel to the magnetic field will accelerate charged particles, one can use the energy of the precipitating particles to estimate the parallel potential difference. Note, however that in practice this can be difficult because particle precipitation indeed occurs particularly during active times and in many different locations such that the conclusions are not straightforward. It is, however, important to note that the energy of precipitating particles is usually in the range of a few keV such that the parallel "potentials" are typically much smaller than the polar cap potential. Note also that the term parallel potential may actually not be correct because it implies a time-independent magnetic field which on the relevant time scales is likely not the case. One can still compute the integral of $E_\parallel$ along magnetic field lines (and would still get particle acceleration) but the electric field is not a potential field. In fact precipitation in discrete auroral arcs is often highly localized in layers (discrete arcs) of widths down to about 100 m.

The simple model of time average or steady magnetospheric convection has been relatively successful. For instance radar observation of the ionospheric flow show the enhancement of the polar cap potential during periods of southward IMF and are used to study the transport of magnetic flux in the magnetosphere. Similar radar observations on the nightside have provided interesting new insight into the convection during the expansion phase. Until recently it was believed that ionospheric convection increases at expansion phase onset because fast flow and enhanced convection is observed in the magnetotail. However, Superdarn radar observation show actually the opposite. Convection appears to slow down at onset and increases gradually over the course of about 10 minutes to about the growth phase level [*Bristow et al.*, 2001; *Bristow et al.*, 2003].

This observation is remarkable because it not consistent with the assumption of a steady state or it implies that the satellite observations in the magnetotail are incorrect. The solution to the inconsistency is simple. The large scale magnetosphere is not in a steady state. Therefore the assumption that the ionospheric electric field provides an instantaneous map of magnetospheric convection is incorrect. During the growth phase convection continues in the ionosphere in the midnight sector. This is not surprising because the ionospheric flow is incompressible and therefore has to continue somehow.

Finally it is worth to note that the ionosphere can have significant influence on the magnetospheric dynamics. Strong ionization (due to precipitation) can increase the ionospheric conductivity by orders of magnitude. The enhanced conductance causes an almost ideal reflection of Alfvén waves which imposes a strong friction on the magnetospheric flow [*Kan*, 1998]. Similarly it is now well established that ion outflow of heavy ions from the ionosphere can exert considerable drag in the magnetosphere.

10.2 Magnetospheric Substorms

Auroral Substorm

Magnetospheric Substorm

Magnetotail Dynamics

Magnetospheric substorm are major events in the magnetosphere. During a substorm a large amount of energy is first stored in the magnetosphere with a subsequent fast release of this energy. A typical substorm consists of three distinct phases:

- The growth phase during which energy is accumulated mostly in the magnetotail.
- the expansion phase during which energy is released, and
- the recovery phase during which the magnetosphere returns mostly to its original state.

Sometime the phrases auroral substorm or magnetospheric substorm are used. The main distinction between these terms is the observational emphasis. The term auroral substorm refers more to the specific auroral signatures and sequence of events. These were historically recognized before the role of the magnetosphere as a whole was realized.

10.2.1 Growth Phase

Typical for almost all substorms is an initial southward turning of the IMF. Due to the southward IMF there is enhanced reconnection on the dayside magnetopause and magnetic flux is removed from the dayside and accumulated in the lobes of the magnetosphere. This corresponds to the storage of magnetic energy in the lobes of the magnetotail. The physical consequences of this process are well documented. The typical duration for the growth phase is 30 to 60 minutes. Typical observations:

- Southward turning of the interplanetary magnetic field (IMF)
- Change (Intensification) of ionospheric convection with typical polar cap potential of 60 kV
- Gradual increase of the size of the polar cap and equatorward expansion of the so-called trapping boundary (boundary that separates hard/energetic particle precipitation of about 10 keV from more discrete and softer precipitation poleward of the boundary)
- Slow increase of the magnitude of the magnetotail lobe magnetic field.
- Slow intensification of the field-aligned current systems (Birkeland currents).
- Stretching of the near-Earth magnetic field at about 6 to 15 R_E from a dipolar to a more tail-like geometry.
- Formation and expansion of a thin near-Earth current sheet (was more rapid thinning toward the end of the growth phase.
- convergent motion of the most equatorward discrete arc and the diffuse aurora equatorward of the trapping boundary.

Not all of the listed properties occur at every substorm growth phase. For instance the size/strength of the polar cap, lobe magnetic field, and Birkeland currents depend also on history. The listed properties are more typical for individual substorms whereas the behavior for a series of substorms may vary. Also while there is a clear statistical correlation to southward IMF there are some (few) substorms where the magnetic field has a small northward and large y component of the IMF.

Let us now set the observation in context to the physics of the growth phase. For southward IMF reconnection increases at the dayside magnetosphere. This is documented by in-situ satellite observations of reconnection at the dayside magnetopause and is consistent with the increase in the ionospheric convection from the day- to the nightside which is nicely documented by an array of superdarn incoherent scatter radars in the northern ad the southern hemisphere.

The increased reconnection implies that the amount of open magnetic flux increases (unless reconnection in the tail is faster in closing magnetic flux) which is equivalent to the increase in the size of the polar cap. The trapping boundary can be considered as a boundary between the strongly dipolar magnetic field and the stretched outer magnetosphere. Within the dipolar magnetosphere precipitation occurs by pitch angle scattering of energetic particles into the loss cone. The fact that the trapping boundary expands equatorward is expected because the amount of open magnetic flux increases such that the amount of dipolar magnetic flux should decrease. The increase of the Birkeland currents has several origins. The southward IMF implies a stronger current at the dayside magnetopause part of which maps into the ionosphere. Similarly the increase of the lobe magnetic field is equivalent to a

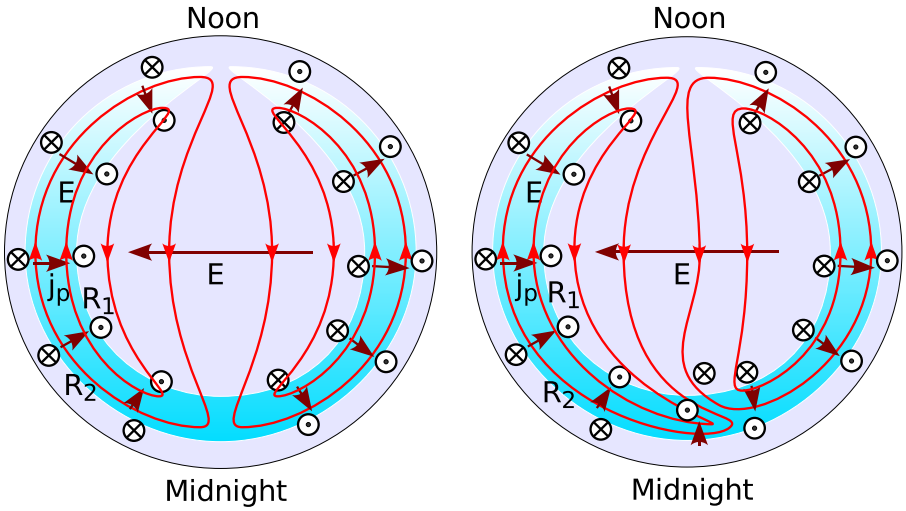

Figure 10.7: Illustration of ionospheric convection (red - potential and streamlines) the associated electric fields $\mathbf{E}$ and Peterson currents $\mathbf{j}_p$ (dark arrows), and the upward (out of the ionosphere) and downward (into ionosphere - circles with x) field aligned currents. The poleward ring of currents is the region 1 current system and the equatorward current is addressed as region 2. The left plot show a typical configuration whereas the plot on the right shows the deformation and intensification of the midnight flow and currents during substorms.

stronger cross tail current in the tail current sheet and a part of this also maps into the ionosphere. Last not least the increased current can also be inferred from th faster magnetospheric convection. A larger cross polar cap potential implies larger electric fields in the ionosphere and thus a larger Peterson current due to

$$\mathbf{I}_p = \underline{\underline{\Sigma}}_p \cdot \mathbf{E}$$

Since the Peterson current must be closed through field-aligned currents, it is clear that the Birkeland current should increase with increased ionospheric convection.

Finally let us consider the magnetotail dynamics. As mentioned a frequently used model for magnetospheric convection is to assume steady state convection. With the knowledge of the cross polar cap potential and the approximate dayside reconnection rate we can estimate the convection needed in the plasma sheet to support a steady magnetic flux transport. Assuming steady magnetotail convection corresponding to 60 kV over 20R_E requires an electric field of about $E_y = 0.5$ mV/m. Using this value in a Tsyganenko magnetic field we can compute the $\mathbf{E} \times \mathbf{B}$ drift velocity in the equatorial plane (Figure 10.8). Note that only velocities close to the noon midnight meridian should be used because it is not clear what the influence of 3D effects is. In any case the figure demonstrates that velocities in excess of 500 km/s are expected tailward of 28 R_E and greater than 100 km/s tailward of 16 R_E. However, the growth phase is a time of typically very slow convection in magnetotail which contradicts the estimated velocities based on a steady state assumption. The conclusion must be that the steady state assumption is not applicable.

The reason for the absence of fast flows are constraints on magnetospheric convection. To formulate these constraints we do not need to solve the fulls set of MHD equations. We have already illustrated that locally mass and entropy p/ρ^γ are conserved. Defining the differential flux tube volume as

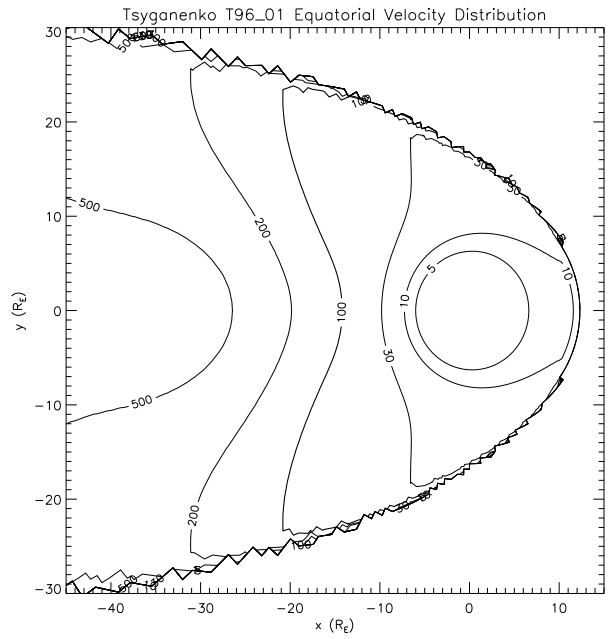

Figure 10.8: Convection velocity in the equatorial plane based on the T96 magnetic field model and a convection electric field of $E_y = 0.5$ mV/m.

$V = \int_F dl/|B|$ and integrating over the full length of a magnetic flux tube with a small cross section it is easy to demonstrate that the number of particles in a magnetic flux tube

$$N = \int_F \frac{ndl}{|B|}$$

and the so-called specific entropy of a flux tube

$$H = p^{1/\gamma} V = \int_F \frac{p^{1/\gamma} dl}{|B|}$$

are conserved during ideal MHD convection, i.e., provided that frozen-in condition applies and for scales larger than c/ω_{pi}:

$$\begin{aligned} \frac{dN}{dt} &= 0 \\ \frac{dH}{dt} &= 0 \end{aligned}$$

Figure 10.9 shows the contour lines of the specific entropy in the equatorial plane for a typical magnetic field configuration based on the T96 Tsyganenko model. This demonstrates that a flux tube convecting from about 40 R_E to about 10 R_E has an entropy by a factor of about 40 larger then typical a 10 R_E. Conservation of entropy for the convected flux tube requires

$$p_{10} V_{10}^{\gamma} = p_{40} V_{40}^{\gamma}$$

such that $p_{10} = p_{40}\,(V_{40}/V_{10})^{\gamma} \approx 2 \cdot 10^3 p_{40}$. However the actual pressure at 10 R_E that is required for the equilibrium is on by a factor of about 30 larger then at 40 R_E. This pressure catastrophe has been used to demonstrate that adiabatic convection from 40 to 10 $R_E$is not possible. This finding is also supported by direct observational statistics which demonstrate that both the number density and the specific entropy are different in the mid and near Earth tail.

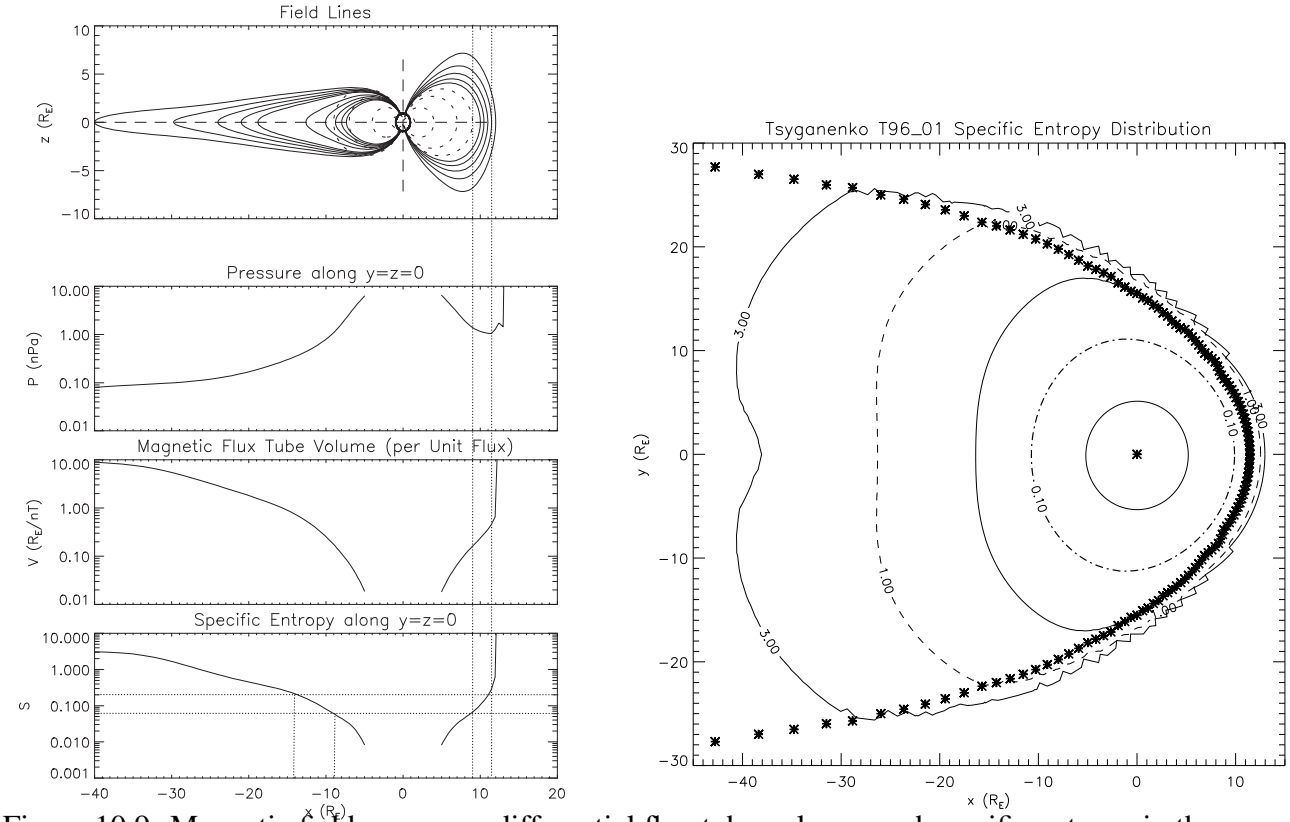

Figure 10.9: Magnetic field, pressure, differential flux tube volume, and specific entropy in the noon midnight meridian (left) and specific entropy mapped into the equatorial plane (right).

The conclusion is that while convection transports flux to the tail lobes and leads to increased compression (and convection) toward the plasma sheet, a corresponding Earthward convection is not possible and not observed during the growth phase, i.e., the convection electric field is largely shielded from the plasma or current sheet. This also implies that the tail magnetic field undergoes a change that is qualitatively sketched in Figure 10.10.

The thinning of the near Earth current sheet occurs inside of about 15 R_E. Satellite observations show that the magnetic geometry of this region is changing from dipolar to a stretched tail-like configuration as illustrated in Figure 10.10. The thickness of the current sheet in this region (and most pronounced at about 10 R_E) decreases gradually [*Pulkkinen et al.*, 1994; *Sergeev et al.*, 1990]. Some observations report an explosive thinning during the last minutes of the growth phase [*Ohtani et al.*, 1992] meaning that during this time the thickness decreases rapidly. The reported current sheets are often only 500 to about 1000 km thick representing a collapse of the current sheet to 2 to 3% of its original width. In the midnight ionosphere the distance between the most equatorward discrete arc and the diffuse aurora (at the equator boundary of the auroral oval) decreases.

The current sheet thinning is of major importance for the subsequent evolution because it provides the conditions for the instability that leads into the growth phase. As pointed out above the onset of

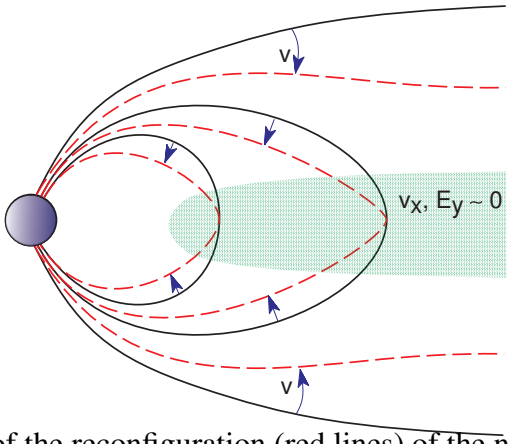

Figure 10.10: Sketch of the reconfiguration (red lines) of the near Earth magnetotail.

dayside reconnection cannot simply generate stationary convection. Note that simple compression due to enhanced lobe field can reduce the current sheet thickness only by a rather small amount for realistic parameters. One model for the current sheet thinning suggests that micro-turbulence generate a diffusion of the thermal pressure [*Lee et al.*, 1998]. This pressure diffusion implies for the equilibrium a different pressure distribution on magnetic flux tubes $p\,(A_y)$ and since the equilibrium current density is $\sim dp/dA_y$ this can have profound implications for the evolution of the current sheet.

Another very promising model using quasistatic models finds that even small boundary perturbations can change the resulting equilibrium properties considerably up to the extend that equilibria seize to exist for some perturbations [*Birn and Schindler*, 2002; *Schindler and Birn*, 1999, 2002]. According to this model the formation and strength of current sheets in the magnetotail does not only depend on the magnitude of the perturbations but also on the temporal history of how the perturbation is applied [*Birn et al.*, 2003].

The specific entropy provides another clue for the current sheet thinning. Figure 10.9 shows a map of the specific entropy obtained from a Tsyganenko magnetic field model. Considering the removal of magnetic flux on the dayside this flux has to be replaced from the nightside. The entropy map shows that convection from a region at about 10 R_E in the tail can replace magnetic flux which has been removed by reconnection from the dayside magnetosphere. Thus the the near Earth tail represents a magnetic flux reservoir from which flux is removed during the growth phase as illustrated in Figure 10.11.

Reconnection with about 60 kV over a period of 45 minutes leads to the transport of $1.5 \cdot 10^8$W. With an average field strength of 50 nT at 10 R_E distance this flux covers an area of about 75 R_E^2 or a strip which could be 5 R_E wide and 15 R_E long. We therefore conclude that a rather significant amount of magnetic flux must have been removed from the near Earth tail.

It is conceivable that this mechanism contributes to the current sheet thinning because it can explain the location of the current sheet thinning and the approximate duration of the growth phase. Recent three-dimensional simulation results (F. Hall, thesis) demonstrate that this mechanism can indeed operate and explain the current sheet thinning on the observed time scale and in the observed location.

Finally let us consider the convergent motion of the most equatorward discrete arc and the diffuse aurora. During the total growth phase this motion may not be continuous but may imply newly formed discrete aurora closer to the trapping boundary and the diffuse aurora. For some substorms the most equatorward discrete arc (which brightens at expansion phase onset) may be only several 10 km poleward of the diffuse aurora at expansion phase onset. The details on auroral arc formation are

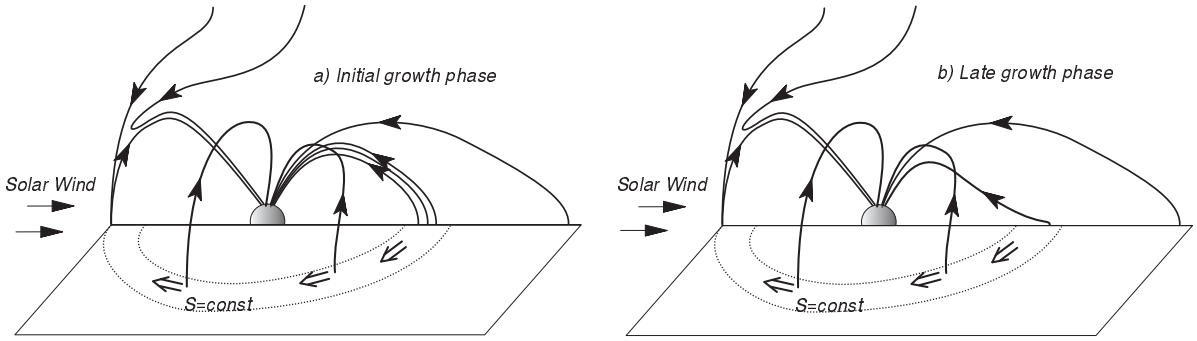

Figure 10.11: Sketch of convection from the tail to the dayside magnetopause.

still unresolved and a topic of ongoing research. However, it makes sense to assume that the location of the most equatorward discrete arc is close to the inner edge of the plasma sheet or better current sheet. In the plasma sheet prior to the growth phase the transition from a tail-like configuration to the strongly dipolar field consists of magnetic flux between roughly 8 to 15 R_E spanning several hundred km when mapped into the ionosphere. The removal of the large amount of magnetic flux from the near Earth current sheet during the growth phase basically implies that the thin current sheet forms forms several (3 to 5 R_E) closer to the Earth than the pre-existing current sheet. Mapped into the ionosphere this implies that the boundary between the discrete aurora and the diffuse aurora should become thinner by several 100 km (Note a difference of 1 R_E at an L shell of 10 translates into about 100 km distance in the ionosphere for a dipole magnetic field)

10.2.2 Expansion Phase

The expansion phase of a substorm is the phase in which previously stored energy is released [*Akasofu*, 1964; *McPherron*, 1979]. The name expansion phases originates from auroral observations. In these observations the most equatorward discrete arc starts to brighten and the auroral activity is expanding rapidly poleward and westward (westward traveling surge). The duration of the expansion phases is typically 30 to 60 minutes, however, with strong activity for about 15 minutes. In summary typical ionospheric observation of the expansion phase show

- Onset: sudden brightening of the most equatorward discrete arc in the pre-midnight sector
- Subsequent poleward and westward expansion of discrete aurora
- Strong increase in the auroral electrojet (a strong hall current in the ionosphere which provides the main magnetic perturbations measured on the ground) and
- A correspondingly strong intensification of the Region 1 and region 2 Birkeland currents.

Basically at the same time there a highly characteristic in-situ satellite observations in the magnetosphere:

- Rapid dipolarization (return to a dipolar magnetic field configuration) in the near Earth magnetotail. This dipolarization is often explained by a disruption of the cross-tail current, however, one should keep in mind that current and magnetic field are equivalent and one should not

interpret the local disappearance of the cross-tail current as a physical mechanism for the reformation of the dipolar field.

- Geosynchronous satellites measure significant increases in the energetic particle fluxes (particle injection).
- In the mid and far tail satellites observe signatures of large plasma bulges (plasmoids) traveling down-tail. Plasmoids are accompanied by fast tailward plasma jetting down-tail.
- Closer to Earth the formation of plasma jets usually toward the Earth.
- Frequently a transient compression and a subsequent decrease of the lobe magnetic field strength.

In recent years much discussion focused specifically on the onset mechanism. Earliest signatures of the onset include the brightening of the onset arc, dipolarization, particle injection, and fast plasma flows. The appearance of these signatures can be measured in some cases within one minute of each other and any one of these signatures can be the first. A precise timing of a particular sequence of these signatures proved rather difficult because they occur very localized and spread over time such that a spacecraft has to be exactly in the correct location to observe the earliest signature.

The mechanism for the onset of the expansion phase is not known. For a long time the ion tearing mode was a major candidate for the onset. However, in a thick current sheet with a normal magnetic field component this mode is strongly stabilized. This changes in the light of strong current sheet thinning. However, it could also be that the current sheet formation leads to a loss of the equilibrium or that the thin current sheets are unstable to either micro-instabilities or to shear-flow (KH type) instabilities. All of these mechanism can more easily operate in a thin current sheet. There is evidence that a significant fraction of onsets is triggered by northward turnings of the IMF. However, it is yet not clear whether the resulting change in convection contributes to the trigger or whether the northward turning just provides a nonlinear perturbation for a marginally unstable current sheet.

Despite the discussion on the onset mechanism the subsequent events are mostly well explained by magnetic reconnection as illustrated by the simulation results in Figure 3.10 [*Birn*, 1980; *Birn and Hones*, 1981; *Otto et al.*, 1990; *Hesse and Birn*, 1991]. The simulation is carried out for the equilibrium shown in Figure 9.4. The figure shows the onset of reconnection and the formation of a plasmoid which is ejected tailward. The plasmoid has a core of enhanced plasma density and pressure. While the plasmoid is traveling down-tail the lobe field is temporarily compressed and after the passage of the plasmoid it settles back to a smaller than initial value because the plasmoid has removed some of the magnetic flux. Fast tailward plasma flow is observed down the tail while there is some enhanced Earthward flow in the near Earth region. The magnetic field close to the Earthward boundary becomes much more dipolar (large z component) because reconnection increases the flux through the equatorial plane Earthward of the x line. Finally the appearance of energetic particle fluxes a geostationary orbits is due to adiabatic particle motion. During the growth phase the magnetic field was relatively weak in this region. Particle on reconnected field lines convect toward the Earth into a region of much stronger magnetic field. The conservation of the magnetic moment $\mu = mv_\perp^2/2B$ for these particles implies that the perpendicular energy can increase by several orders of magnitude depending on the original and final field strength. This process is called betatron acceleration and can indeed explain the observed increase in energetic particle in the near Earth region [*Birn et al.*, 1997].

It should also be noted that magnetic reconnection not only can explain these various observations but that it is required in the expansion phase. During the growth phase a large amount of closed magnetic

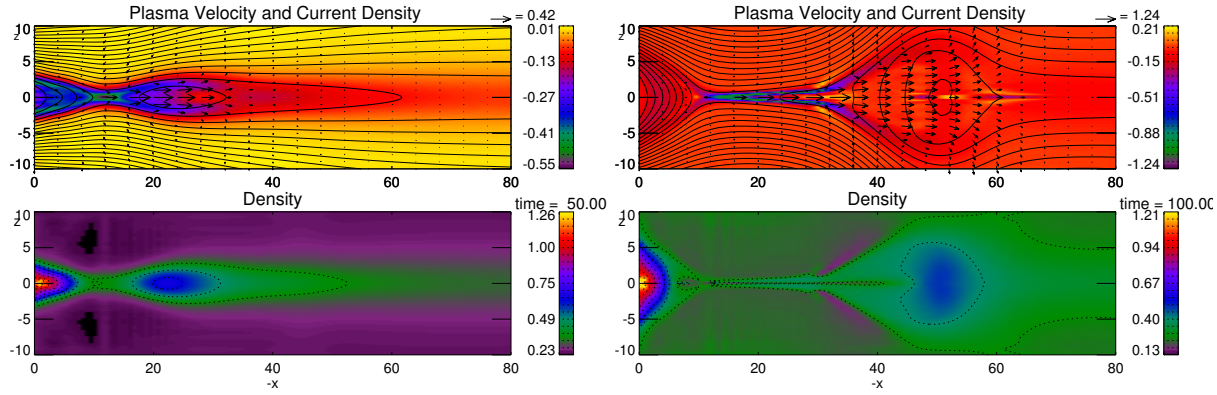

Figure 10.12: Results from a two-dimensional MHD simulation of reconnection in the magnetotail.

flux has been opened. The only mechanism by which this flux can be closed again is reconnection in the magnetotail.

The ionospheric signatures follow in part from the magnetospheric evolution. The fact that the most equatorward discrete arc brightens first is often interpreted in the sense that something happens at the thin current sheet. Whether this is the onset of an instability or the loss of an equilibrium is not known. Some research proposes that the configuration of the thin current current sheet becomes unstable to the ballooning instability (an ideal interchange instability in which fingers of strong earthward and tailward convection develop close to the current sheet. In any case the subsequent westward and poleward expansion agrees qualitatively well with magnetic reconnection because reconnection in the tail implies that increasingly magnetic flux mapping to higher latitudes is reconnected.

Due to the fast flow in the tail one would expect a further increase of convection in the ionosphere. However, surprisingly this does not seem to be the case. While the region 1 and 2 currents strongly intensifies (and therefore also the Peterson and Hall currents) the electric field in the ionosphere (and the polar cap potential) do not change significantly. In fact at expansion phase onset the ionospheric velocities appear to decrease slightly. The reason for this is the strong increase in density through precipitation. This is illustrated by assuming an ionization of Δn neutrals with a momentum $m\Delta n\mathbf{v}_n$ and the original plasma momentum $mn\mathbf{v}_0$. Total momentum conservation:

$$m(n+\Delta n)\mathbf{v} = mn\mathbf{v}_0 + m\Delta n\mathbf{v}_n$$

which yields a plasma bulk velocity after the ionization of

$$\mathbf{v} = \frac{n}{n+\Delta n}\mathbf{v}_0 + \frac{\Delta n}{n+\Delta n}\mathbf{v}_n$$

Since Δn can be 10 times n and the neutral velocity can be small compared to the plasma velocity the convection velocity could be reduced by a factor of 10 during the ionization (depending on time scales). The timescale for recovery of the plasma flow can be rather high because the Peterson conductance can be $\sum_p$ several 10 to several 100 Siemens yield a reflection coefficient of ≥ 0.9 which implies of order 10 Alfvén bounce times to re-accelerate the ionospheric flow! Thus that the ionospheric conductance increases strongly and this increase accounts mostly for the strong increase in ionospheric currents.

Qualitatively this provides a reasonable and consistent picture of substorm expansion, however, there are still many important unresolved questions. Among the most important of these are

- What is the detailed physics of discrete auroral arc formation (and particle acceleration), and what is the influence of particle precipitation on MI coupling.
- What is the physics of the so-called diffusion region in magnetic reconnection in the magnetotail.

10.2.3 Recovery Phase and Other Related Phenomena

The recovery phase completes the substorm sequence and is the return of the magnetospheric configuration to its original configuration. The duration is typically 1 to 2 hours. During the recovery phase the auroral oval is dimming and the aurora moves back to higher latitudes. Typical are pulsating patches of auroral and quiet arcs reappear. Similarly the current sheet and plasma sheet returns to its original size.

This does not mean that the recovery phase is entirely understood. An important unresolved question is the origin of the plasma sheet material or in other words how the plasma sheet is reformed.

It should also be mentioned that the recovery phase can be rather brief or entirely absent. During prolonged periods (many hours) of southward IMF with many substorms there is often not a complete return to a pre-substorm state of the magnetosphere. Similarly there may not be a clearly identifiable growth phase during such times.

10.2.4 Steady Magnetospheric Convection

In particular during prolonged periods of relatively steady southward IMF there is a state of the magnetosphere which is termed steady magnetospheric convection events (SMC's) [*Sergeev et al.*, 1996]. Note that this term should not be taken literally in the mathematical sense. During SMC's there is continuous reconnection at the dayside magnetopause. Typical for SMC's are so-called bursty bulk flows (BBF's) [*Angelopoulos et al.*, 1992]. These are events which show several minutes of very fast plasma flow which can be tail- or Earthward. Bursty bulk flows can actually occur all times, however, usually rather infrequent. During SMC's, BBF's are very frequent, the aurora is highly active, and the auroral electrojet is strong. Intuitively it is conceivable that BBF's are localized reconnection events in the magnetotail in particular because magnetic flux must be re-closed in the tail and transported back to the dayside. Although there is considerable auroral activity the large scale organized release of energy as observed in substorms is absent for SMC's. Thus the magnetosphere has two different ways to respond to the same IMF and solar wind conditions. Why it would respond one way or the other is unresolved.